

Multi-Domain Finite Element Meshing for Parotid Acinar Cell Modeling and Simulation

John Rugis^{a,b} Nathan Pages^b James Sneyd^b David Yule^c

^acorresponding author - email: j.rugis@auckland.ac.nz, phone: 649-373-7999

^b Department of Mathematics, University of Auckland, Auckland, New Zealand

^cSchool of Medicine and Dentistry, University of Rochester, Rochester, NY, USA

May 15, 2017

Keywords

multi-domain meshing, volumetric mesh, finite element modeling, parotid acinar cells.

Abstract

350 words maximum.

1 Introduction

The primary role of salivary gland acinar cells is to secrete saliva, the lack of which causes a host of severe medical difficulties [FvdVS⁺85, Mel91]. Thus, an understanding of the mechanisms underlying saliva secretion are vital for the understanding of oral health. The basic mechanism of saliva secretion is well understood [Nau92], and has been previously modeled in detail [STAB⁺03].

However, although much is understood about saliva secretion, important questions, both experimental and

theoretical, remain. From the theoretical point of view, one of the most interesting questions is how the structure of the acinar cells affects the properties of the Ca^{2+} waves. Along these lines, we have previously reported our first simulation results obtained using an anatomically accurate three-dimensional parotid acinar cell model [SMZ⁺17]. In that initial investigation, we modeled single, non-coupled cells. In this paper, we build on that work, extending our model to multiple (seven), coupled cells.

MORE HERE? Why extend to coupled cells?

2 Design Considerations

We have been using a straightforward implementation of the Finite Element Method (FEM) [Goc06, Hug, Gos05] for our three-dimentional parotid cell simulations and continue doing so in this latest work. In keeping with relatively common FEM practice, we model the surface of each cell with a triangle mesh, then fill-in the cell interiors with tetrahedrons, which results in a complete volumetric mesh for each cell. In the meshes that we developed for our prior work the cells did not physically contact each other i.e. there was a physical gap between the cells.

We have recently extended our modeling to include interactions between adjacent cells and this imposed additional demands on our mesh construction. With our new design, each cell now touches one or more other cells, sharing some portion of it's surface. We have chosen to model adjacent cell surfaces with *conformal faces* in which triangle mesh faces are shared in common between adjacent cells. Note that this facilitates a fairly straightforward mathematical implementation of the interactions between cells. Because we still need to keep track of what's going on in each cell independently, the overall mesh is thought of as being *multi-domain* (one domain for each cell).

As with our prior work, the source data for our acinar cell mesh construction consists of a calibrated confocal microscopy image stack.

CITE YULE?

3 Description of Method

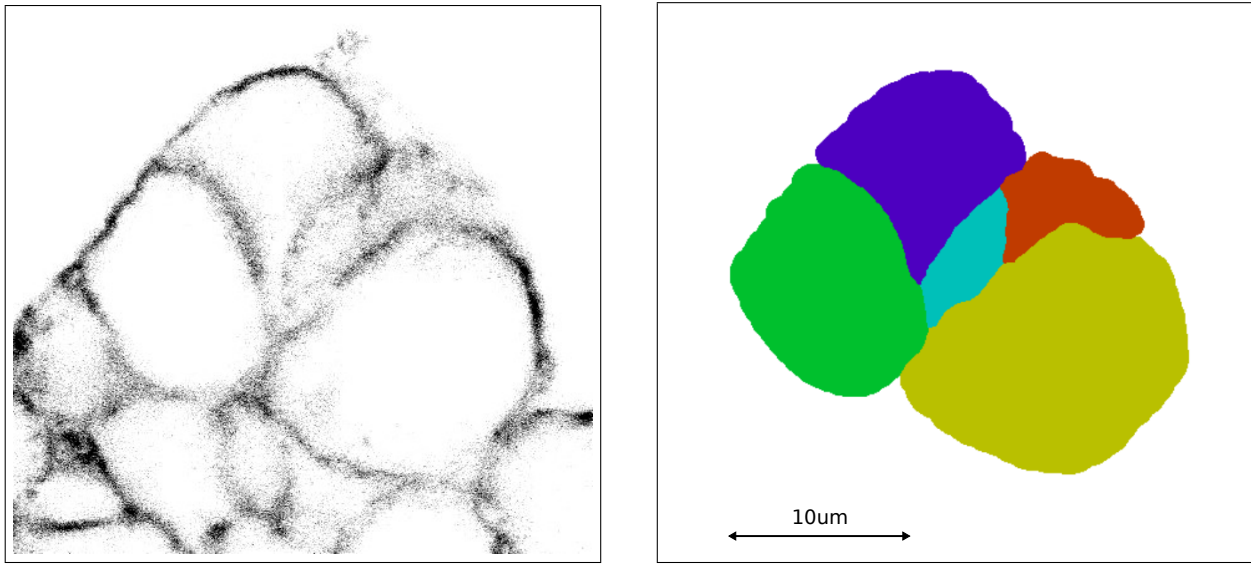


Figure 1: Subsection of a microscopy image slice on the left and its segmentation on the right.

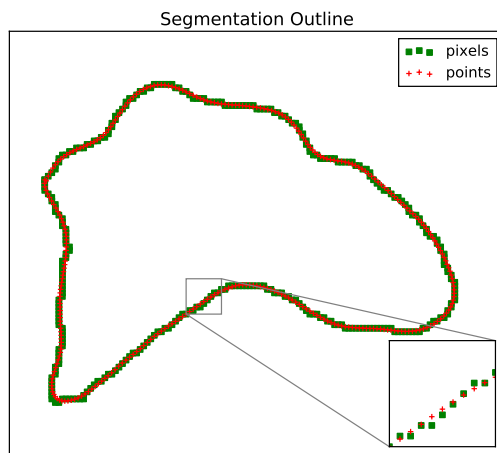


Figure 2: A sample segmentation pixel outline in green with smoothed node points in red.

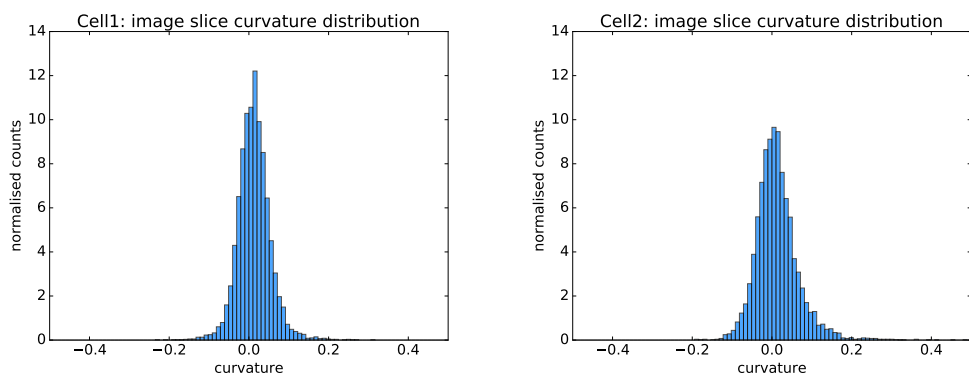


Figure 3: Reference curvature histograms for two of the cells.

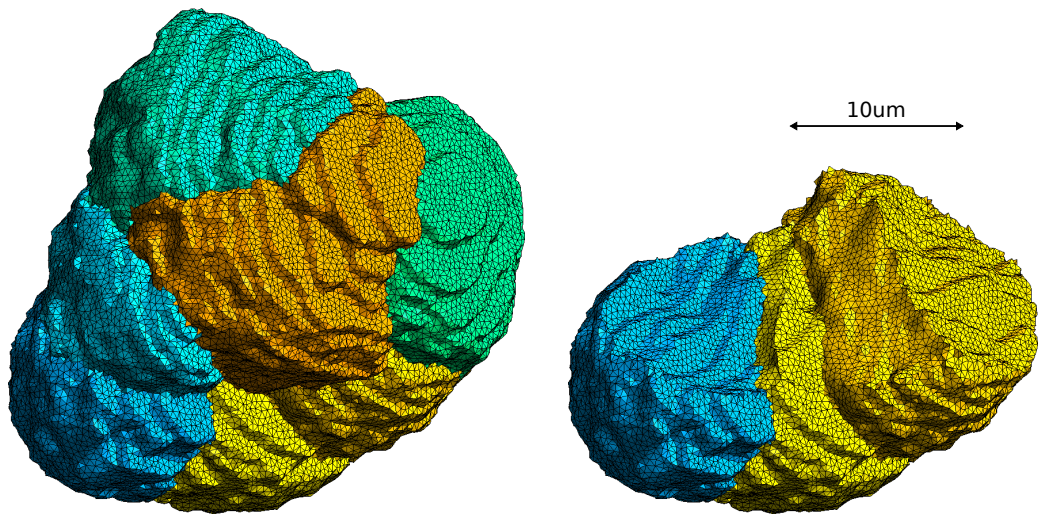


Figure 4: Rough multi-domain surface mesh: all seven cells (left) and three exposed cells (right).

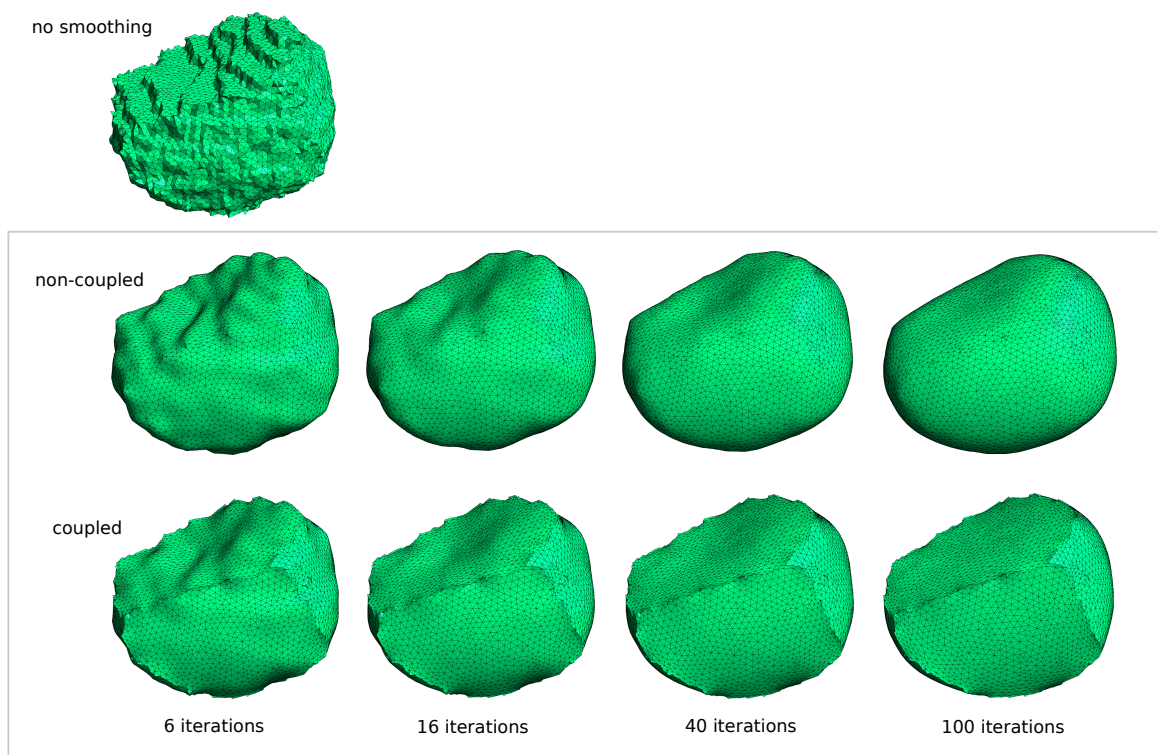


Figure 5: Cell smoothing evolution, with and without inter-cell coupling.

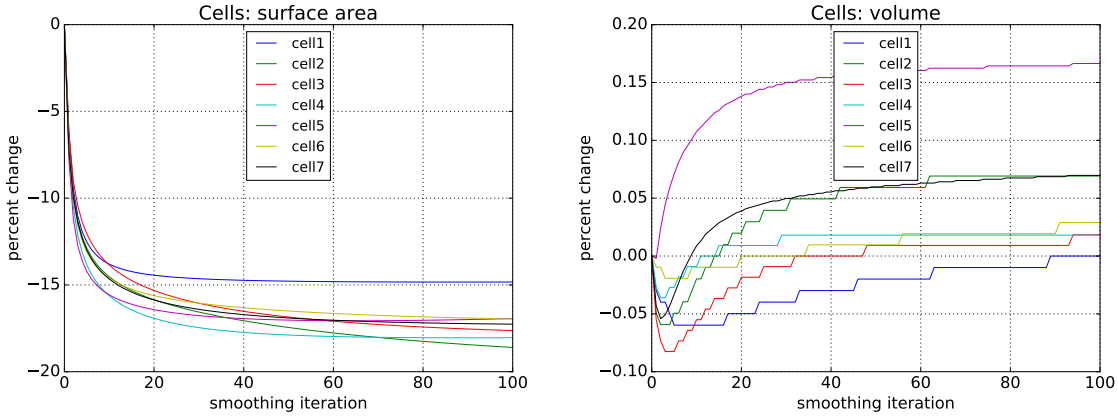


Figure 6: Cell surface area and volume evolution over one hundred coupled smoothing iterations.

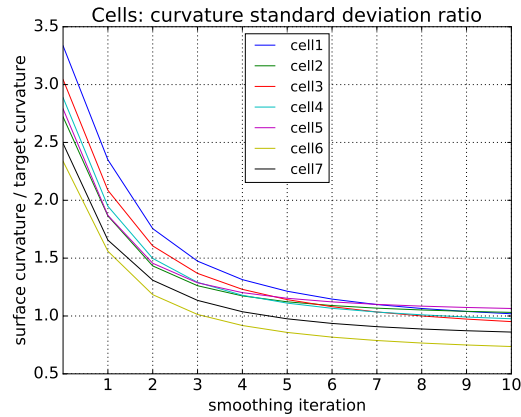


Figure 7: Half of the cells hit the target curvature standard deviation ratio of one after ten iterations.

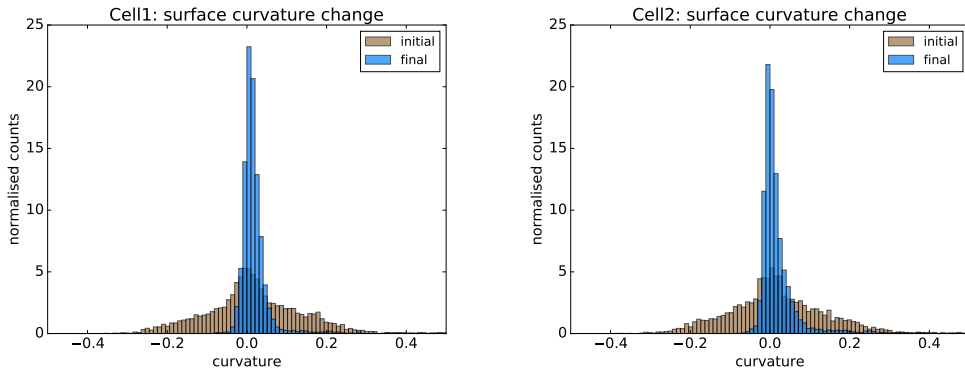


Figure 8: Initial surface curvature distribution in brown and smoothed surface curvature in blue.

4 Results

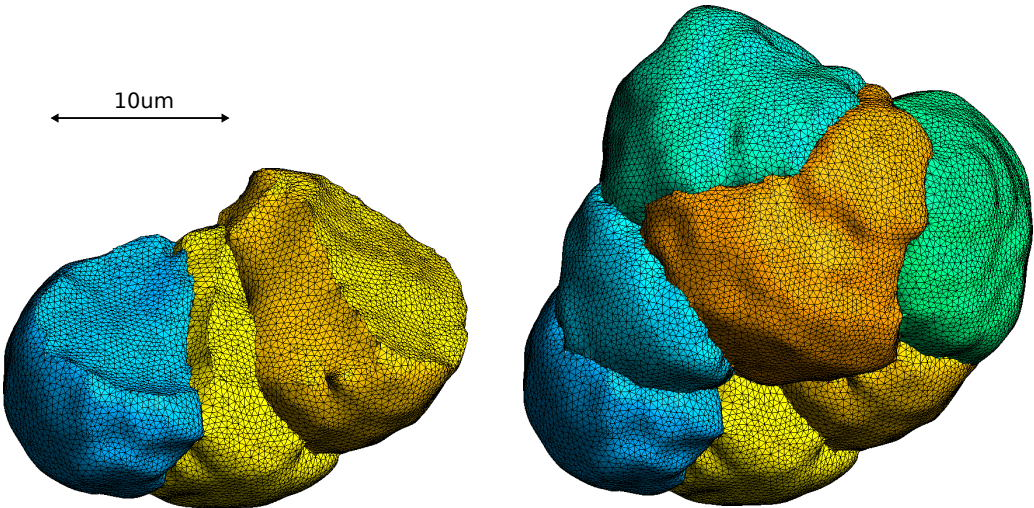


Figure 9: Fully meshed smoothed cells: three exposed cells (left) and all seven cells (right).

5 Discussion

6 Conclusion and Future Plans

7 Acknowledgements

This work was supported by the National Institutes of Health grant number 5R01DE019245 and by a grant from New Zealand eScience Infrastructure (NeSI).

References

- [FvdVS⁺85] P C Fox, P F van der Ven, B C Sonies, J M Weiffenbach, and B J Baum. Xerostomia: evaluation of a symptom with increasing significance. *J Am Dent Assoc*, 110(4):519–25, Apr 1985.
- [Goc06] Mark S Gockenbach. *Understanding and implementing the finite element method*. Siam, 2006.
- [Gos05] Michael R Gosz. *Finite element method: applications in solids, structures, and heat transfer*. CRC Press, 2005.
- [Hug] Thomas J. R. Hughes. *The Finite Element Method: Linear Static and Dynamic Finite Element Analysis*. Dover Publications.

- [Mel91] J E Melvin. Saliva and dental diseases. *Curr Opin Dent*, 1(6):795–801, Dec 1991.
- [Nau92] B Nauntofte. Regulation of electrolyte and fluid secretion in salivary acinar cells. *Am J Physiol*, 263(6 Pt 1):G823–37, Dec 1992.
- [SMZ⁺17] James Sneyd, Shawn Means, Di Zhu, John Rugis, Jong Hak Won, and David I. Yule. Modeling calcium waves in an anatomically accurate three-dimensional parotid acinar cell. *Journal of Theoretical Biology*, 419:383 – 393, 2017.
- [STAB⁺03] J Sneyd, K Tsaneva-Atanasova, J I E Bruce, S V Straub, D R Giovannucci, and D I Yule. A model of calcium waves in pancreatic and parotid acinar cells. *Biophys J*, 85(3):1392–405, Sep 2003.

A Numerical Data

cell	curvature std
1	0.0412
2	0.0538
3	0.0432
4	0.0491
5	0.0555
6	0.0602
7	0.0544

Table 1: The standard deviation of the curvature values (in μm^{-1}) for each cell obtained from the microscopy image stack.

cell	0	1	2	3	4	5	6	7	8	9	10
1	0.1374	0.0968	0.0723	0.0607	0.0541	0.0500	0.0472	0.0453	0.0439	0.0428	0.0411
2	0.1464	0.1003	0.0771	0.0679	0.0631	0.0604	0.0587	0.0574	0.0566	0.0560	0.0555
3	0.1315	0.0901	0.0694	0.0591	0.0531	0.0493	0.0467	0.0447	0.0432	0.0420	0.0411
4	0.1418	0.0957	0.0736	0.0634	0.0579	0.0546	0.0524	0.0508	0.0496	0.0487	0.0480
5	0.1549	0.1037	0.0808	0.0714	0.0667	0.0640	0.0623	0.0611	0.0602	0.0596	0.0591
6	0.1407	0.0939	0.0713	0.0610	0.0552	0.0516	0.0492	0.0475	0.0461	0.0451	0.0443
7	0.1355	0.0901	0.0712	0.0617	0.0564	0.0531	0.0509	0.0494	0.0483	0.0475	0.0468

Table 2: The evolution of standard deviation of mean surface curvature for the seven cells (in μm^{-1}) at each coupled smoothing iteration.

cell	0	1	2	3	4	5	6	7	8	9	10
1	628.64	590.17	569.09	559.23	553.53	549.84	547.26	545.37	543.93	542.80	541.90
2	729.06	680.85	657.39	646.44	639.76	635.12	631.65	628.91	626.66	624.77	623.15
3	681.01	638.45	619.64	609.78	603.46	598.93	595.46	592.68	590.37	588.40	586.70
4	712.88	661.36	637.82	626.19	619.08	614.15	610.47	607.57	605.02	603.22	601.52
5	443.18	408.76	393.58	386.72	382.76	380.16	378.30	376.90	375.81	374.92	374.19
6	684.72	636.81	615.75	605.50	599.26	595.00	591.87	589.46	587.55	585.98	584.67
7	627.42	582.15	564.89	555.74	549.94	545.88	542.82	540.42	538.47	536.84	535.46

Table 3: The evolution of surface area for the seven cells (in μm^2) at each coupled smoothing iteration.

cell	0	1	2	3	4	5	6	7	8	9	10
1	1004.3	1004.0	1003.9	1003.9	1003.8	1003.7	1003.7	1003.7	1003.7	1003.7	1003.7
2	1012.4	1011.9	1011.8	1011.8	1011.8	1011.9	1011.9	1012.0	1012.0	1012.1	1012.2
3	1090.2	1089.6	1089.4	1089.3	1089.3	1089.3	1089.4	1089.4	1089.5	1089.5	1089.6
4	1105.7	1105.4	1105.3	1105.3	1105.4	1105.4	1105.5	1105.5	1105.6	1105.6	1105.6
5	492.76	492.75	492.88	492.98	493.05	493.11	493.16	493.20	493.23	493.26	493.29
6	1036.3	1036.2	1036.2	1036.1	1036.1	1036.1	1036.1	1036.1	1036.1	1036.2	1036.2
7	903.99	903.60	903.50	903.53	903.60	903.69	903.78	903.87	903.94	904.01	904.07

Table 4: The evolution of volume for the seven cells (in μm^3) at each coupled smoothing iteration.